

Pd Catalysts

Preparation of Secondary Phosphine Oxide Ligands through Nucleophilic Attack on Imines and Their Applications in Palladium-Catalyzed Catellani Reactions

Chan-Yu Hu,^[a] Ya-Qian Chen,^[a] Guan-Yu Lin,^[a] Ming-Kai Huang,^[a] Yu-Chang Chang,^[a] and Fung-E Hong^{*[a]}

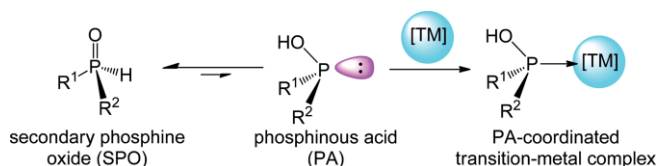
Abstract: Several new amino-type secondary phosphine oxide (SPO) pre-ligands (**3a–3h**) that contain P–N bonds were synthesized and characterized. SPOs **3a–3h** can tautomerize to phosphinous acids (PA, **3a–3h**) as genuine ligands. The formation of SPOs **3a–3h** occurred first through nucleophilic attack on the imine carbon atom, then by the addition of RPCl_2 ($\text{R} = \text{Ph}$, Cy , $t\text{Bu}$, or $i\text{Pr}$), and work-up under acidic conditions. The P–N bond in the newly prepared SPOs is evident from the crystal structures of SPOs **3d** and **3h**. Reactions of SPOs **3f**, **3g**, or **3h** with $\text{Pd}(\text{COD})\text{Cl}_2$ ($\text{COD} = \text{cyclooctadiene}$) yielded palladium complexes **6f**, **6g**, or **6h**. In these crystal structures, PAs **3f**, **3g**, and

3h act as didentate ligands through P and N donors. Intriguingly, the reaction of SPO **3f** with $\text{Pd}(\text{COD})\text{Cl}_2$ also gave rise to palladium complexes **7fa**, **7fb**, and **8f**. The crystal structures of **7fa** and **7fb** show that the palladium atom is chelated by PA **3f** and coordinated by a phosphine-like ligand fragmented from SPO **3f** through C–N bond dissociation. Finally, the syntheses of carbazole derivatives were pursued in Catellani reactions with SPOs **3g** and **3h** as pre-ligands. A mechanism is proposed to account for the catalytic reaction (see the Supporting Information). The optimized conditions for Suzuki reactions using selected SPO ligands are also reported.

Introduction

For many years, the various shapes and functions of trisubstituted phosphines have been the favorite choice for ligand-assisted transition-metal-catalyzed reactions.^[1] Nevertheless, these types of phosphines are mostly vulnerable to oxidation,^[2] which lessens their bonding capacities toward low-valence transition metals.^[3] This severe drawback limits their extensive application as authentic soft ligands towards soft metals in coordination. It is also not a desirable character for the long-term storage of some precious phosphine compounds. One way to resolve this obstacle is to allow phosphine to be partially oxidized and maintain its coordinating capacity until it is needed. Phosphinous acid [PA, $\text{P}(\text{OH})\text{R}^1\text{R}^2$], a tautomeric form of its corresponding air-stable secondary phosphine oxide [SPO, $\text{O}=\text{P}(\text{H})\text{R}^1\text{R}^2$] in solution, is thus a potential candidate and has the capacity to act as a legitimate phosphine ligand in the coordination of transition metals (Scheme 1).^[4] Since the first synthesis of di-*n*-alkylphosphine oxides in 1952, various kinds of SPOs have been prepared in the past several decades and their stabilities towards air and moisture have also been validated.^[5,4a] Moreover, their capabilities as effective ligands in transition-

metal-catalyzed cross-coupling reactions have also been evaluated and reported elsewhere.^[6,4d,4f–4u]



Scheme 1. Process for the conversion of a secondary phosphine oxide (SPO) to its corresponding tautomeric form, phosphinous acid (PA), and the onward formation of a PA-coordinated metal complex.

Besides its commonly formulated simple $\text{O}=\text{P}(\text{H})\text{R}^1\text{R}^2$ format, recently designed secondary phosphine oxides come in various shapes and forms. Pfaltz and Helmchen reported an authentic bidentate ligand that was formed by incorporating an imine moiety into the SPO framework [Figure 1(a)].^[7] Recently, Ackermann demonstrated that some N–P–N-type secondary phosphine oxides (or heteroatom-substituted secondary phosphine oxides, HASPOs) could behave as excellent ligands in various

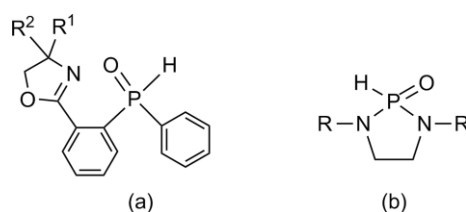
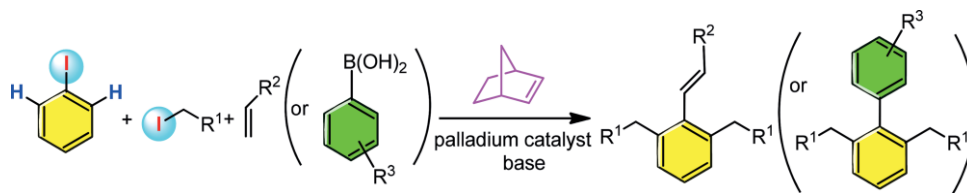


Figure 1. Two categories of secondary phosphine oxides.

[a] Department of Chemistry, National Chung Hsing University, 250 Kuo-Kuang Road, Taichung 40227, Taiwan
E-mail: fehong@dragon.nchu.edu.tw
<http://www.nchu.edu.tw/~chem/fehong.htm>

Supporting information for this article is available on the WWW under <http://dx.doi.org/10.1002/ejic.201600181>.



Scheme 2. Catellani-type Heck and Suzuki reactions.

catalytic reactions [Figure 1(b)]. By combining with a suitable palladium salt, these HASPOs worked well for Suzuki–Miyaura reactions as well as amination reactions, even reactions starting from inactive aryl chlorides.^[8] Upon deprotonation, Cramer et al. showed that this N–P–N-type SPO could act as hemilabile ligand that binds Ni⁰ and Al^{III} in the asymmetric Ni-catalyzed hydrocarbomoylation of alkenes.^[9]

Recently, phosphines containing P–N bonds in their scaffolds have attracted much attention. It is believed that the phosphorus atom in this type of phosphines is significantly electron-rich than those without the P–N bond, a characteristic that is beneficial to the oxidative addition process in the commonly seen cross-coupling catalytic cycles.^[10]

In addition, cross-coupling reactions are well-known processes for their efficiencies in joining two separate components, in particular, for the formation of carbon–carbon bonds from the corresponding aryl or alkyl reactants.^[11] Nevertheless, these methods are limited by their scopes in only combining two substances at a time. For further incorporation of a third substance to the coupled compound, more step(s) must be taken. It would be advantageous if three reactants could be coupled in the same reaction, for example, in a one-pot reaction.

One of the most attractive multiple-component reactions was reported in the mid-1980s by Italian chemist M. Catellani and was later coined as the “Catellani reaction”.^[12] At first glance, the reaction seems not to have many differences from the conventional cross-coupling reaction (Scheme 2). Nevertheless, this type of reaction deliberately promotes the C–H activation process of Ar–I at its *ortho*-position and leads to the replacement of *ortho*-hydrogen atoms by an alkyl or aryl group, which indeed is a fascinating achievement. As seen, C–H activation has been the target for extensive studies recently.^[13] The Catellani reaction can readily achieve C–H activation of the *ortho*-hydrogen atom(s) of aryl halides (mostly aryl iodide). It is worth noting that norbornene plays an indispensable role as co-catalyst to promote the targeted route for the reaction. Determined by the final elementary step, Catellani developed the corresponding Catellani-type Heck and Suzuki reactions, which result in the production of the targeted products after C–H activation processes.^[14]

In their early works, Catellani et al. did not use any ligand as an auxiliary, and the amount of palladium catalyst used was up to 20 %.^[14b,15] Later, Lautens and co-workers employed some of well-chosen ligands for the reactions and achieved better performances.^[16] Nevertheless, the role played by conventional ligands such as phosphines remains doubtful in this type of reactions. Ever since the disclosure of the original Catellani reaction, there have been many interesting reports aimed at delving

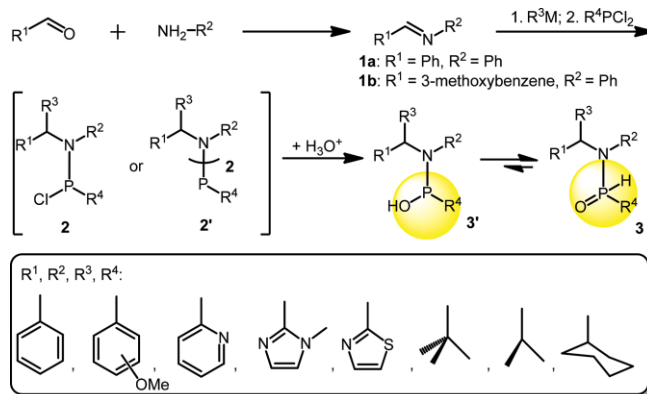
more deeply into the mechanism of this type of reactions and thereby improving the catalytic performances.^[17] As studies on SPO-assisted Catellani-type reactions are rare, it is of interest to us to explore the roles played by SPO-type phosphine ligands in this type of reactions.

Herein, we report the preparation of several new amino-based secondary phosphine oxides, which contain P–N bonds in their frameworks. Their capacities as mono- or bidentate ligands in several palladium-catalyzed Catellani reactions were evaluated. The structures of several fascinating SPO-ligated palladium complexes with unique bonding modes will be discussed as well.

Results and Discussion

Preparation of Amino Secondary Phosphine Oxides 3a–3h

Several amino secondary phosphine oxides, **3a–3h**, were prepared and characterized by spectroscopic methods (Scheme 3, Figure 2). The general procedure for the preparation of the compounds is presented as follows. Initially, imines **1** were prepared from each corresponding aldehyde and amine. Subsequently, treatment of imines **1** first through nucleophilic attack on the imine carbon atom, followed by the addition of PhPCl₂ thus led to the formation of each matching phosphinamines (**2** or **2'** for disubstituted products). Finally, conversion of **2** into each of the corresponding phosphinous acids **3'** was achieved through hydrolysis in acidic media. In solution, a tautomeric equilibrium can exist between the secondary phosphine oxide **3** and its phosphinous acid **3'** under ambient conditions. Nor-



Scheme 3. Preparation of amino secondary phosphine oxides. Substituents R on the four positions could be: phenyl, 3-methoxyphenyl, 2-methoxyphenyl, 4-methoxyphenyl, pyridyl, 2-methyl-1H-imidazolyl, thiazole, *tert*-butyl, isopropyl, cyclohexyl.

mally, the former is more favorable in the absence of highly electron-withdrawing substituent(s). The distinctly large coupling constant ($J_{\text{P,H}} = 450\text{--}600\text{ Hz}$) indicates the presence of a $\text{P}(\text{H})=\text{O}$ fragment in the secondary phosphine oxide.

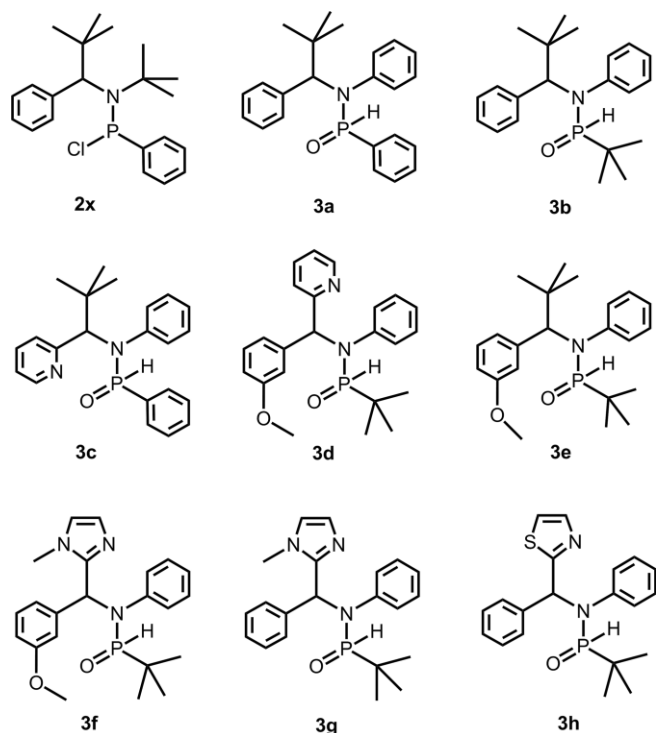


Figure 2. Secondary phosphine oxides, **3a–3h**, and chlorophosphine **2x**.

It was found that the hydrolysis of each **2** species indeed led to the formation of each corresponding SPO **3a–3h** except for **2x**. The existence of a $\text{P}(\text{H})=\text{O}$ fragment in **2x** is evident from the determination of its crystal structure by X-ray diffraction methods (see the Supporting Information, Figure S1). To our delight, the crystal structures of **3d** and **3h** were resolved (Figure 3). The existence of a double bond between $\text{P}(1)$ and $\text{O}(2)$ in **3d** is evident from its short bond, $1.4839(13)\text{ Å}$. The bond angles of

$\text{O}(2)\text{--P}(1)\text{--N}(1)$, $\text{O}(2)\text{--P}(1)\text{--C}(19)$, and $\text{N}(1)\text{--P}(1)\text{--C}(19)$ are $117.42(8)^\circ$, $113.62(8)^\circ$, and $108.63(8)^\circ$, respectively. Clearly, a pseudo-tetrahedral environment surrounds the phosphorus atom. The major structural features of **3d** are also true for **3h**.

Reactions of Amino Secondary Phosphine Oxide **3f** with Palladium Salts

The fact that imidazole moieties exhibit coordination capacity towards palladium through the N(imidazole) site has been demonstrated elsewhere.^[6c] Thereby, compound **3f** (or **3g**, **3h**) is expected to have the potential to act as a bidentate ligand through both the P(phosphine) and N(imidazole) sites.

Here, **3f** was selected to react with various palladium sources, PdX_2 ($\text{X} = \text{Cl}, \text{Br}$), $\text{Pd}(\text{COD})\text{X}_2$ ($\text{COD} = \text{cyclooctadiene}$), $\text{PdCl}_2(\text{CH}_3\text{CN})_2$, or $\text{Pd}(\text{OAc})_2$, and the processes were monitored by ^{31}P NMR spectroscopy (Scheme 4). The disappearance of the distinctly large coupling constant, which is caused by the $\text{P}(\text{H})=\text{O}$ bond in the SPO form, is strong evidence for the formation of the phosphinous acid (PA) form and that the compound acts as a phosphine ligand in the palladium complex. The generation of the *cis* (or *trans*) form of bis(phosphine) ligands coordinated to the palladium complex, **4f_{cis}** (or **4f_{trans}**), was expected as the initial and major product by employing PdX_2 ($\text{X} = \text{Cl}, \text{Br}$) as the palladium sources.^[6] In addition, the formation of **5f** is presumed when using $\text{Pd}(\text{OAc})_2$ as the palladium source. To our delight, the crystal structure of **6f** was able to be determined by X-ray diffraction methods (Figure 4). As shown in Figure 4, the SPO **3f** indeed behaves as a bidentate ligand through both the P(phosphine) and N(imidazole) coordinating sites. Similar results were also observed for the reactions of **3g** and **3h** with PdCl_2 [or $\text{Pd}(\text{COD})\text{Cl}_2$]. The major structural features of **6g** and **6h** are analogous to that of **6f**. Indeed, **3g** and **3h** also behave as bidentate ligands (Figure 4).

Moreover, two fascinating isomeric forms of palladium complexes, **7fa** and **7fb**, were also obtained from crystal-growing processes. The crystal structures of **7fa** and **7fb** revealed that **3f** indeed acts as a PN bidentate ligand through both the

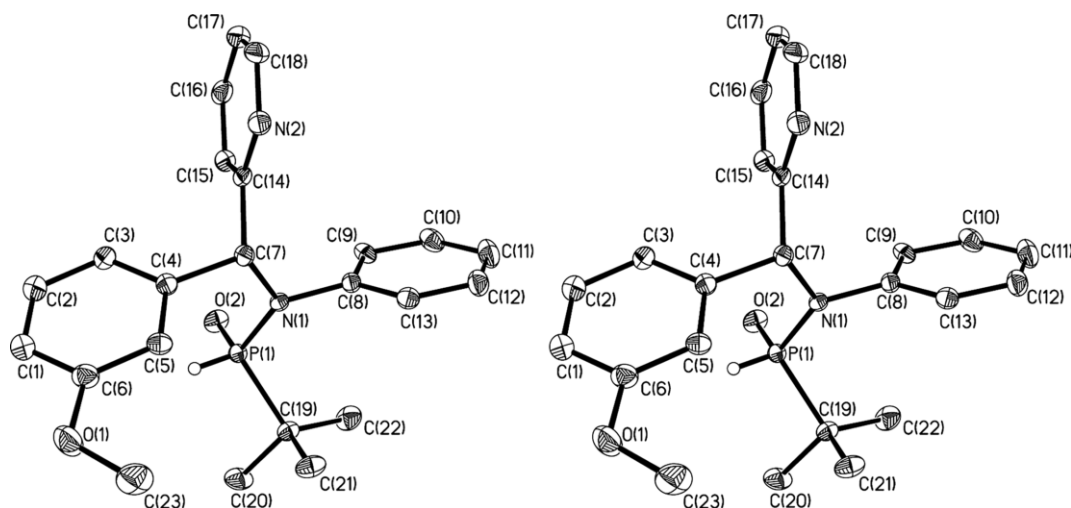
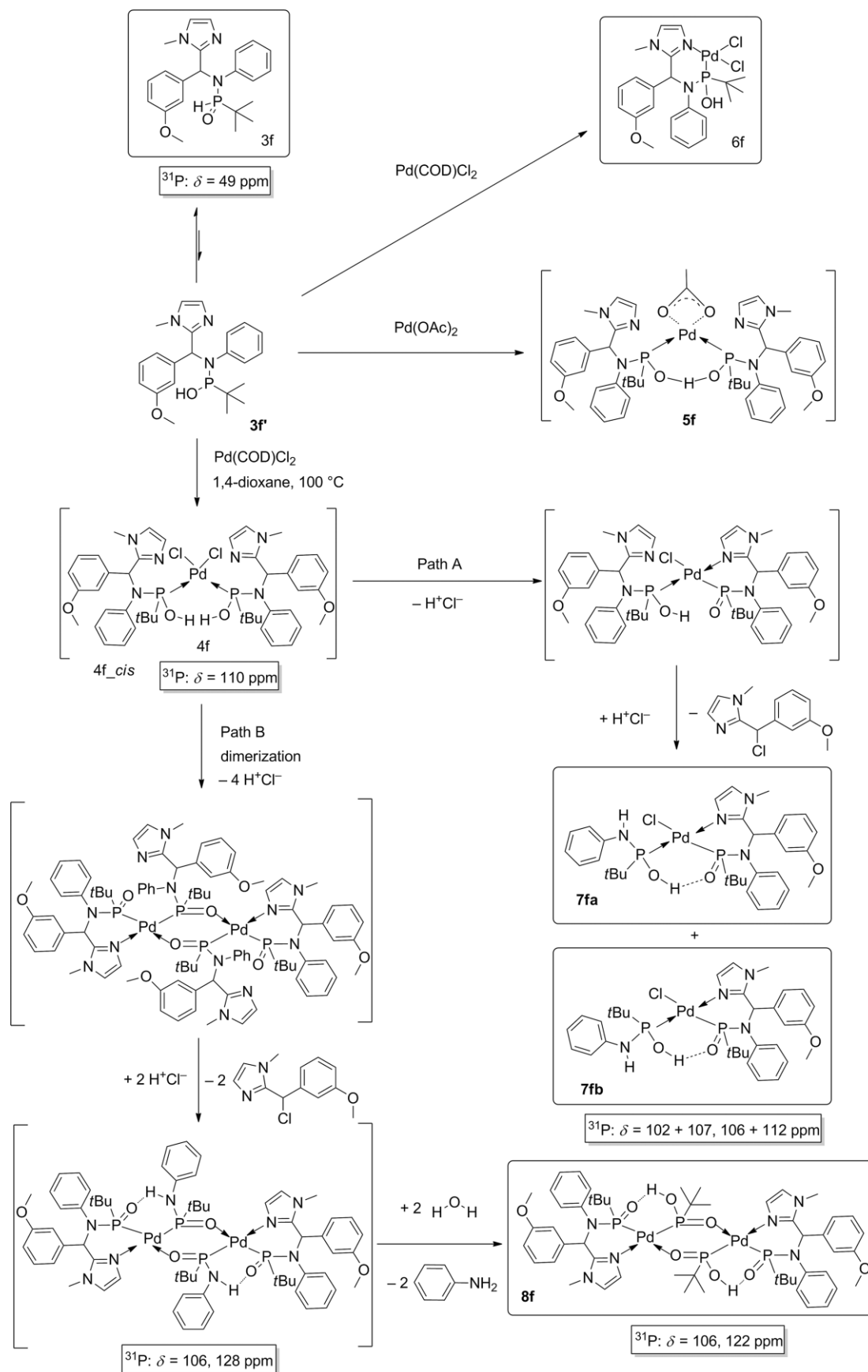


Figure 3. ORTEP drawings of **3d** (left) and **3h** (right).



Scheme 4. Reactions of **3f** with $\text{Pd}(\text{COD})\text{Cl}_2$ and $\text{Pd}(\text{OAc})_2$. The compounds highlighted by boxes were characterized by single-crystal X-ray diffraction methods, whereas those in brackets are presumably reaction intermediates or metastable compounds, which could not be characterized.

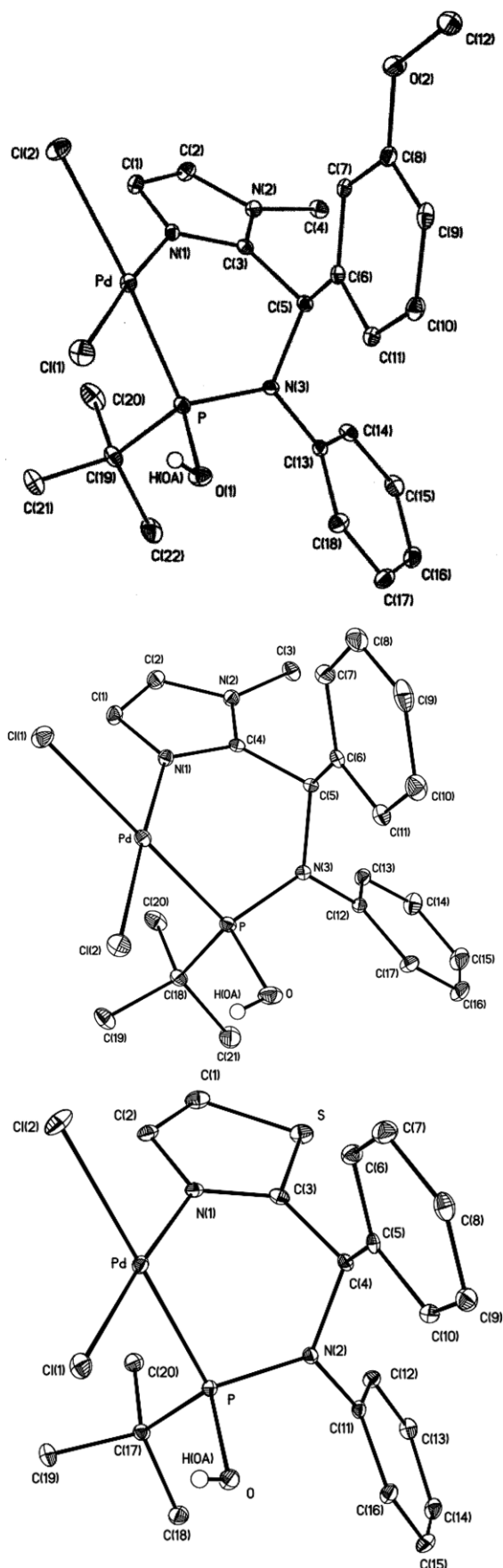


Figure 4. ORTEP drawings of **6f** (top), **6g** (middle), and **6h** (bottom).

P(phosphine) and N(imidazole) sites, like those shown in complex **6f**, yet in a much more complicated manner. The structure of **7fa** shows that there is another fragmented phosphinous ligand, P(OH)(*t*Bu)(NPh), from **3f** that coordinates to palladium as well (Figure 5). Notably, there is intramolecular hydrogen bonding between these two oxygen atoms. The palladium atom resides in a square-planar environment. The process for the generation of **7fa** (or **7fb**) is remarkable and worthy of further examination. Presumably, a bis-**3f**-coordinated palladium dichloride complex **4f_cis** (or **4f_trans**) was initially formed, then one of the coordinated ligands of **4f_cis** (or **4f_trans**) was fragmented into 2-[chloro(3-methoxyphenyl)methyl]-1-methyl-1*H*-imidazole plus one phosphine ligand, 1-*tert*-butyl-1-hydroxy-*N*-phenylphosphanamine, by attack on the N–C bond of the coordinated **3f** by the released proton and chloride. Here, the released proton presumably was released during the formation of intramolecular hydrogen bonding between the two PA-type ligands in **7fa**. It is quite unusual that the strong N–C bond of **3f** is broken rather than the presumably weak P–N bond. The rather similar structure of **7fb** compared to that of **7fa** was resolved by single-crystal X-ray diffraction methods (Figure 5). The only difference lies in the conformation of the monodentate ligand P(OH)(*t*Bu)(NPh). Unfortunately, the quantities of **7fa** and **7fb** were not sufficient to execute other spectroscopic methods than the above-mentioned single-crystal X-ray diffraction methods.

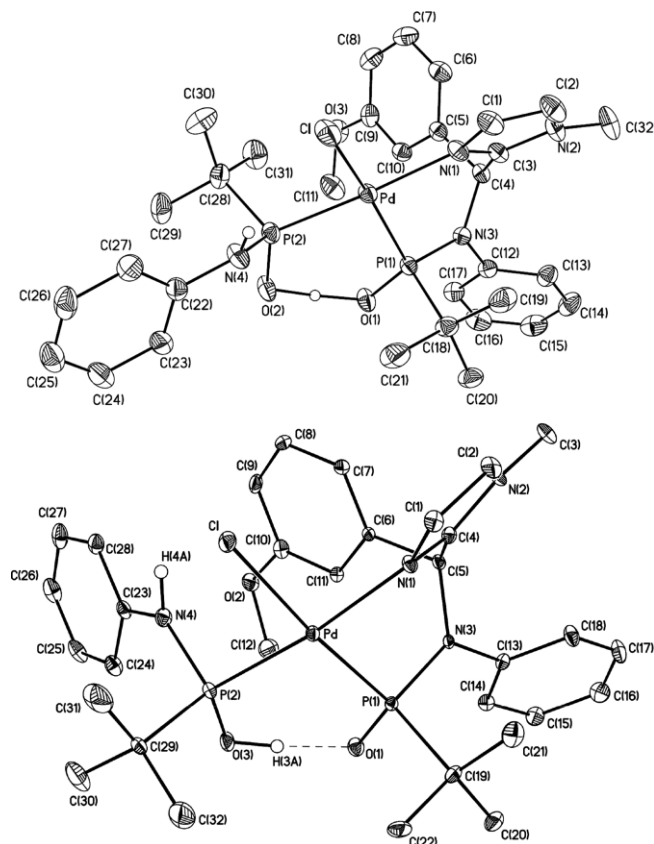
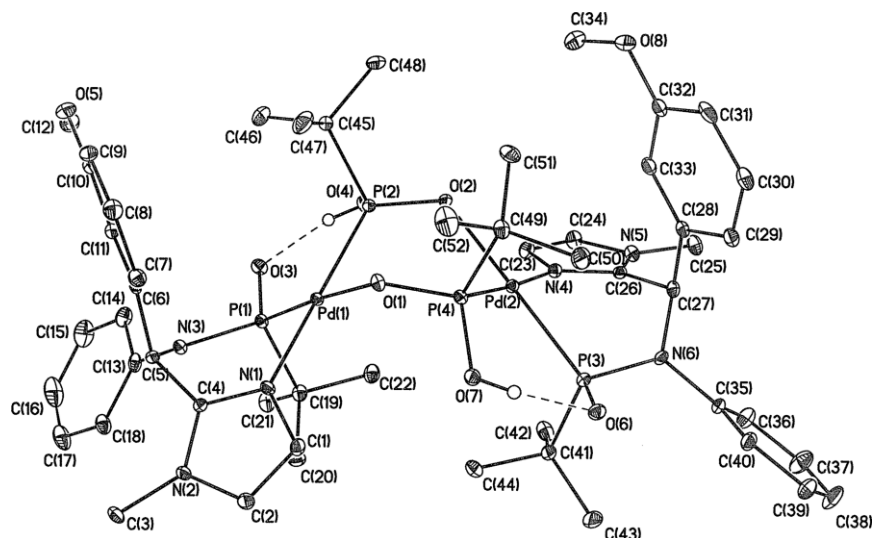


Figure 5. ORTEP drawings of **7fa** (top) and **7fb** (bottom).

Another quite unique palladium complex, **8f**, was also obtained from crystal-growing processes. The crystal structure of

Figure 6. ORTEP drawing of **8f**.

8f (Figure 6) reveals that it is a Pd dimer, albeit without a direct Pd–Pd bond. Rather, the two Pd atoms are bridged by two deprotonated P(tBu)(OH)(O)[−] ligands. The *tert*-butylphosphonous acid, P(tBu)(OH)₂, is believed to derive from the cleavage of the P–N bond of **3f** during hydrolysis, which is different from the previous case, that is, the formation of **7f**, where the N–C bond of **3f** was broken. The core structure of the compound is a six-membered ring, which is more like a boat form than a chair form.^[18] The two chloride atoms are absent from the starting palladium source, PdCl₂. Still, each palladium atom remains in its initial valence state, +2. Two sets of intramolecular hydrogen bonding can be clearly seen. The surrounding environment of Pd(1) is of square-planar geometry. This is also true for Pd(2). Indeed, the structure of **8f** presents a quite unique feature of its own; two sets of peaks in the ³¹P NMR spectra corresponding to four phosphorus atoms are observed in a ratio of 1:1.

Application of Selected Complexes in the Preparation of Carbazoles

Catellani et al. reported a fascinating process for the synthesis of bioactive carbazole derivatives in a one-pot manner. The process utilizes palladium-catalyzed sequential C–C and C–N formations from *ortho*-substituted iodoarenes and *N*-acetylated *ortho*-bromoanilines in the presence of norbornene.^[19] Later, they claimed that the addition of triphenylphosphine (PPh₃) was beneficial for this reaction to achieve significant conversion when using acetamide as one of the reactants. By using the selected SPOs **3** as pre-ligands, results of the optimized reaction conditions for palladium-catalyzed Suzuki–Miyaura reactions are reported along with results for Heck reactions (in the Supporting Information).

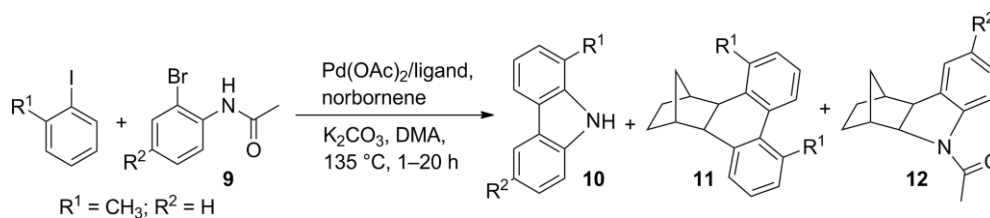
We wondered whether these newly prepared SPOs could be utilized as effective ligands for this catalytic system. Thereby, some of the ligands, **3b** and **3h**, along with two well-known

phosphine ligands, triphenylphosphine and 1,2-bis(diphenylphosphino)ethane (dppe), were selected to combine with Pd(OAc)₂ as catalyst precursors as well as the pre-formed palladium complex **6h**, for this catalytic process. As already revealed in the crystal structure of **6h**, **3h** could act as a P[⊂]N bidentate ligand through both the P(phosphine) and N(imidazole) sites in the coordination of the palladium atom. Therefore, the ratio of Pd/ligand is preset at ca. 1:1 for this type of ligands. By contrast, triphenylphosphine and **3b** are monodentate ligands, and the Pd/ligand ratio is designated as 1:2. The reaction conditions are as follows: 2-iodotoluene (0.2 mmol), *N*-(2-bromophenyl)acetamide (0.4 mmol), base (0.8 mmol), norbornene (0.42 mmol), palladium salt (10 mol-%), ligand (11–22 mol-%), dimethylacetamide (DMA; 2 mL), which were allowed to react at 135 °C for a preset reaction time of 20 h. As shown in Entry 1 (Table 1), a modest conversion was obtained, even in the absence of any phosphine ligand, which is in contradiction to Catellani's previous observation.^[19] In general, the efficiency of the reaction

Table 1. Catellani reaction for the formation of 1-methyl-9*H*-carbazole by employing various ligands.^[a]

Entry	Ligand	Yield [%] ^[b]		
		10	11	12
1	–	39.6 (26.4, 25.9 ^[c])	20.1	21.6
2 ^[d]	3b	46.4 (36.4)	14.7	33.5
3 ^[e]	3h	50.9 (41.1) ^[f]	9.0 ^[f]	21.2 ^[f]
		54.6 (38.6)	16.9	25.1
4	6h	50.5 (37.3)	13.9	33.6
5 ^[d]	PPh ₃	33.6 (23.5)	14.0	26.9
6 ^[e]	dppe	46.6 (35.9)	15.2	36.3
7 ^[g]	PPh ₃	67	–	–

[a] Conditions: 2-iodotoluene (0.2 mmol), *N*-(2-bromophenyl)acetamide (0.4 mmol), norbornene (0.42 mmol), K₂CO₃ (0.8 mmol), Pd(OAc)₂ (10 mol-%), DMA (2 mL), 135 °C, 20 h. [b] Conversion rate was determined by ¹H NMR spectroscopy. Isolated yields are shown in parentheses. [c] DMF was used. [d] Pd/L = 1:2. [e] Pd/L = 1:1. [f] Reaction for 1 h. [g] 2-iodotoluene (1.1 equiv.), *N*-(2-bromophenyl)acetamide (1.0 equiv.), norbornene (0.25 equiv.), Pd(OAc)₂ (5 mol-%), PPh₃ (10 mol-%), K₂CO₃ (2.2 equiv.) in DMF at 105 °C, 48 h.



Scheme 5. Palladium-catalyzed sequential C–C and C–N formations by Catellani-type reactions.

using bidentate ligands seems to be better than those utilizing monodentate ones (Entries 2, 4, 6 vs. 5). There is not much difference when using the pre-formed catalyst precursor against the in situ method (Entry 2 vs. 4). Overall, the application of these newly prepared SPOs in this catalytic system are slightly better than those without them. Note that a much shorter reaction time was needed than that in Catellani's reaction. As shown, the reaction is almost complete within 1 h (Entry 3). No further improvement in yield for the targeted compound could be observed, although there was some alteration in the yields of some side products, **11** and **12** (Scheme 5).

A mechanism is proposed to explain the experimental results for the formation of the three products observed (Supporting Information). The routes for the production of **10** and **11** are proposed in accord with Catellani's work. The observation of **12** is of significant interest to us as there is only the initial acetamide but no iodobenzene fragment incorporated in the structure. There are two catalytic cycles (cycles 1 and 2) as can be seen in section S3 in the Supporting Information that might compete for the consumption of acetamide. Thereby, the reaction was purposely designed by initially setting the ratio of 2-iodotoluene/*N*-(2-bromophenyl)acetamide equal to 1:1 or 2:1. In the former case, only the formation of carbazole **10** was observed. There was no trace amount of **12** detected. By contrast, both carbazoles **10** and **12** were found in the latter case. Thereby, it is safe to say that the rate for the formation of carbazole **10** is much faster than the generation of **12**. It is only after the complete consumption of iodobenzene in the major catalytic cycle that the reaction of *N*-(2-bromophenyl)acetamide started to react with Pd⁰ and led to the production of **12**.

Optimization of Palladium-Catalyzed Suzuki–Miyaura Reactions of Phenylboronic Acid and Various Bromides by Using **3a**, **3b** and **3c** as Ligands

As demonstrated repeatedly, the catalytic performance is always better for an active catalyst precursor, ligand-coordinated palladium complex, with a ratio of 1:2 for monodentate ligand/palladium salt. Initially, the catalytic performances of various combinations of palladium sources and ligands were investigated. The results for the Suzuki–Miyaura coupling reactions using 4-bromoanisole as the substrate are summarized in Table 2. As shown, **3b** stands out as the best ligand among all three SPOs with the combination of Pd(OAc)₂/ligand = 1:2 (Entry 2). It is reasonable to assume that the large steric hindrance of the *t*Bu group in **3b** assists the rate of reductive elimination,

thus speeding up the overall rate of the catalytic cycle. The fact that poor performance was observed in the absence of any ligand indicates that these amino secondary phosphine oxides are indeed beneficial to the catalytic performance (Entry 4). Ligand **3c** was assumed to have the potential to act as a bidentate ligand through the phosphine and pyridyl coordinating sites. Nevertheless, even worse performance was observed when using the combination of Pd(OAc)₂ and **3c** in a 1:1 ratio as the catalytic precursor (Entry 3). Therefore, it is more likely that **3c** behaves as a monodentate ligand in this case.

Table 2. Suzuki–Miyaura coupling reactions of 4-bromoanisole and phenylboronic acid, employing ligands **3a–3c**.^[a]

Entry	Ligand	NMR conv. [%]
1	3a	38
2	3b	> 99
3	3c	52 (41) ^[b]
4	–	25

[a] Conditions: 4-bromoanisole (1.0 mmol), phenylboronic acid (1.5 mmol), KOH (5 mmol), Pd(OAc)₂ (1.0 mol-%), ligand (2.0 mol-%), THF (1 mL), 60 °C, 2 h. [b] [Pd]/**3** = 1:1.

In addition, the ratio of Pd(OAc)₂/**3b** was changed from 1:1 to 1:3 intentionally. Not much difference was observed (Table 3). Therefore, the ratio of Pd(OAc)₂/**3b** was set at 1:2 thereafter.

Table 3. Suzuki–Miyaura coupling reactions of 4-bromoanisole and phenylboronic acid, employing various Pd/L ratios.^[a]

Entry	Pd/L	NMR conv. [%]
1	1:1	> 99
2	1:2	> 99
3	1:3	> 99

[a] Conditions: 4-bromoanisole (0.5 mmol), phenylboronic acid (0.75 mmol), KOH (2.5 mmol), Pd(OAc)₂ (1 mol-%), **3b** (1–3 mol-%), THF (1 mL), 60 °C, 1 h.

As is generally accepted, the starting active catalytic precursor in the Suzuki–Miyaura cross-coupling catalytic cycle is a zerovalent palladium species. Nevertheless, the most commonly used palladium sources are Pd^{II} owing to their resistance to air in long-term storage. Pd(OAc)₂ is prone to be reduced more readily to zerovalent Pd in the presence of electron-rich phosphines than halogenated palladium salts, PdX₂. In addition, its availability, relatively cheap cost, ease of handling, and most of all, its efficiency in cross-coupling reactions makes Pd(OAc)₂ a favorite choice among the various palladium sources. Here, the screening of various available palladium sources was pursued. Interestingly, Pd(OAc)₂ as well as all halogenated palladium compounds had excellent performances with short reaction

times of 1.0 h (Table 4, Entries 1–4). Unexpectedly, relatively poor performance was observed for the zerovalent palladium source, $\text{Pd}_2(\text{dba})_3$ (Entry 5; dba = dibenzylideneacetone). As shown, at least a minimum of 30 min was required for the reduction of the divalent palladium salt to the zerovalent active species. Once the active species is formed, the completion of the reaction can be carried out within 30 min.

Table 4. Suzuki–Miyaura coupling reactions of 4-bromoanisole and phenylboronic acid, employing various palladium sources.^[a]

Entry	Pd source	NMR conv. [%]		
		0.5 h	1.0h	2.0 h
1	$\text{Pd}(\text{OAc})_2$	0	> 99	> 99
2	$\text{Pd}(\text{COD})\text{Cl}_2$	0	> 99	> 99
3	$[\text{Pd}(\text{allyl})\text{Cl}]_2$	0	> 99	> 99
4	PdBr_2	0	> 99	> 99
5	$\text{Pd}_2(\text{dba})_3$	0	84	> 99

[a] Conditions: 4-bromoanisole (1.0 mmol), phenylboronic acid (1.5 mmol), KOH (5 mmol), palladium salt (1.0 mol-%), **3b** (2.0 mol-%), THF (1 mL), 60 °C.

The participation of base in Suzuki–Miyaura coupling reaction is essential for the success of the catalysis. It is also one of the most unpredictable factors. Although the role played by base has been examined theoretically by computational means, careful laboratory examination is unavoidable. Thereby, the impact of employing various bases in the reaction was investigated. As shown in Table 5, KOH (or K_3PO_4) in THF is the most effective among all the bases screened (Entries 1 and 2). Moderate performance was observed when using NaOtBu as base (Entry 3), whereas, the other bases, including K_2CO_3 , KOtBu , and NaOH , performed poorly (Entries 4–6). Unexpectedly, one of the commonly used bases, Cs_2CO_3 , had no effect on the catalytic performance (Entry 7). As shown in Entry 8, no conversion was observed without the presence of base. KOH is chosen as the base thereafter as its performance is even better than that of K_3PO_4 at a lower reaction temperature.

Table 5. Suzuki–Miyaura coupling reactions of 4-bromoanisole and phenylboronic acid, employing various bases.^[a]

Entry	Base	NMR conv. [%]
1	KOH	> 99
2	K_3PO_4	> 99
3	NaOtBu	48
4	K_2CO_3	16
5	KOtBu	12
6	NaOH	6
7	Cs_2CO_3	0
8	–	0

[a] Conditions: 4-bromoanisole (0.5 mmol), phenylboronic acid (0.75 mmol), base (2.5 mmol), $\text{Pd}(\text{OAc})_2$ (1 mol-%), **3b** (2 mol-%), THF (1 mL), 60 °C, 1 h.

For most of cross-coupling reactions, the generation of ionic intermediate(s) is proposed during the catalytic cycle. Thereby, polar solvents are always a favorite choice as the solubility of these species will greatly affect the catalytic performance. As shown in Table 6, the combination of KOH with either THF, 1,4-dioxane, or DMF leads to excellent results in 1.0 h (Entries 1–3). Toluene and DMSO performed poorly (Entries 4 and 5). Even worse performance was observed when using the nonpolar solvent hexane (Entry 6). From these results, THF was chosen as

the optimized reaction solvent as its performance is excellent and it does not undergo self-coupling, such as in the case of DMF. After screening these influential factors, it was found that the optimal reaction conditions are as follows: using **3b**/ $\text{Pd}(\text{OAc})_2$ as the catalyst precursor combined with a KOH/THF system, which are allowed to react at 60 °C for 1 h.

Table 6. Suzuki–Miyaura coupling reactions of 4-bromoanisole and phenylboronic acid, employing various solvents.^[a]

Entry	Solvent	NMR conv. [%]
1	THF	> 99
2	DMF	> 99
3	dioxane	92
4	toluene	20
5	DMSO	7
6	hexane	0

[a] Performed under the same reaction conditions as given in the footnote of Table 5 except for the solvent employed.

Conclusions

Several new air- and moisture-stable amino secondary phosphine oxide pre-ligands (SPOs, **3a–3h**) containing P–N bonds were prepared and applied in palladium-catalyzed Catellani reactions. Eight crystal structures, including those of the two SPOs **3d** and **3h** as well as of the three PA-chelated Pd^{II} complexes **6f**, **6g**, and **6h** were reported. Interestingly, two isomeric palladium complexes, **7fa** and **7fb**, with fascinate structures were obtained from the reaction of **3f** with $\text{Pd}(\text{COD})\text{Cl}_2$. Complexes **7fa** and **7fb** are isomers, and the palladium atom in each isomer is coordinated by a newly formed PA ligand of $\text{P}(\text{OH})(\text{tBu})(\text{NHPh})$ through C–N bond dissociation of **3f**. As to the crystal structure of **8f**, the two bridging ligands, $\text{P}(\text{tBu})(\text{OH})(\text{O})^-$, could be fragments resulting from C–N and P–N bond dissociations of **3f**. The Catellani-type reactions for the productions of carbazoles also yielded valuable organic compounds through unexpected routes. By using 4-bromoanisole as the substrate, the selected SPO ligands were employed to find the optimized conditions for palladium-catalyzed Suzuki and Heck reactions (see the Supporting Information).

Experimental Section

General: All reactions were carried out under nitrogen by using standard Schlenk techniques or in a nitrogen-flushed glovebox. Freshly distilled solvents were used. All processes for separations of the products were performed by Centrifugal Thin Layer Chromatography (CTLC, Chromatotron, Harrison model 8924) or column chromatography. GC–MS analysis was performed with an Agilent 5890 gas chromatograph (Restek Rtx-5MS fused silica capillary column: 30 m, 0.25 mm, 0.5 μm) with an Agilent® 5972 mass-selective detector. Routine ^1H NMR spectra were recorded with a Varian-400 spectrometer at 399.756 MHz. The chemical shifts are reported in ppm relative to the internal standard TMS ($\delta = 0.0$ ppm). ^{31}P and ^{13}C NMR spectra were recorded at 161.835 and 100.529 MHz, respectively. The chemical shifts for the former and the latter are reported in ppm relative to the internal standards H_3PO_4 ($\delta = 0.0$ ppm) and CHCl_3 ($\delta = 77$ ppm), respectively. Mass spectra were recorded with a JOEL JMS-SX/SX 102A GC/MS/MS spectrometer. Electrospray-ionization high-resolution mass spectra (ESI-HRMS)

were recorded with a Finnigan/Thermo Quest Mat 95 XL mass spectrometer. The deviations of the experimental values from the theoretical predictions in the elemental analysis for compounds were presumably caused by encapsulated solvents, CH₂Cl₂, THF, H₂O. Therefore, HRMS of these compounds have been provided to validate the identities of them (see Figure S5).

Synthesis and Characterization of 3a–3h: Benzaldehyde (10.2 mL, 100 mmol) (or picolinaldehyde, 9.5 mL, 100 mmol), aniline (9.1 mL, 100 mmol), and H₂O (25 mL) were added into a 250 mL round-bottomed flask. The solution was then stirred at 25 °C for 3 h. The resulting organic layer was extracted with ethyl acetate and saline solution. Then, it was dried with anhydrous MgSO₄. A dark-yellow solid **1a** (17.2 g, 95.0 mmol, 95 %) or **1e** (17.3 g, 95.0 mmol, 95 %) was obtained after the solvent had been removed under vacuum. Without further purification, **1a** (1.08 g, 6.0 mmol) or **1e** (1.08 g, 6.0 mmol) was placed into a 250 mL round-bottomed flask with a side arm and magnetic stirrer. The air in the flask was removed and replaced by nitrogen. THF (15 mL) was added and the solution was cooled to –78 °C. Then, *t*BuLi (3.6 mL, 7.2 mmol) was added slowly to the solution along the flask wall. The mixed solution was then stirred for 1 h before it was warmed up to 25 °C. Meanwhile, PhPCl₂ (0.36 mL, 3.0 mmol) or *t*BuPCl₂ (0.48 g, 3.0 mmol) dissolved in THF (2 mL) was prepared for addition to the flask. The solution was cooled to –78 °C again before PhPCl₂ or *t*BuPCl₂ in THF was slowly added. After stirring for an additional 1 h, presumably compound **2a** (or **2e**) was formed. Without further purification, 3 N HCl was added to the solution at 0 °C, which was stirred for another 1 h. The organic layer was extracted twice with ethyl acetate. Then, it was dried with anhydrous MgSO₄. A dark-yellow solid **3a** (0.16 g, 0.45 mmol, 15 %) was obtained by column chromatography. The yields of **3b** and **3c** were 25 % (0.26 g, 0.75 mmol) and 33 % (0.36 g, 0.99 mmol), respectively. A similar procedure was carried out for the preparation of **3e** except for starting with 3-methoxybenzaldehyde rather than benzaldehyde. The yield of **3e** was 21 % (0.24 g, 0.63 mmol). As for the preparation of **3f**, the nucleophile was the deprotonated 1-methyl-1*H*-imidazole (by *n*BuLi), and the yield of **3f** was 17 % (0.20 g, 0.51 mmol). For the preparation of **3d**, the nucleophile was the deprotonated 2-bromopyridine, and the yield was only 3 % (0.035 g, 0.09 mmol). Similar procedures might be carried out for the syntheses of **3g** and **3h** except for using deprotonated imidazole and thiazole as nucleophiles. The yields of **3g** and **3h** were 11 % (0.116 g, 0.316 mmol) and 18 % (0.660 g, 1.78 mmol), respectively.

Spectroscopic Data for 3a: ¹H NMR (CDCl₃): δ = 7.91 (d, *J*_{PH} = 474 Hz, 1 H), 7.66–7.61 (m, 1 H), 7.46–7.43 (m, 2 H), 7.34–7.24 (m, 10 H), 6.53–6.51 (dd, *J* = 6.4, 2.0 Hz, 2 H), 4.07 (d, *J*_{PH} = 6.80 Hz, 1 H, P-H), 0.93 (s, 9 H) ppm. ¹³C NMR (CDCl₃): δ = 150.9, 139.9, 132.1, 132.0, 130.8, 130.7, 128.7, 128.6, 128.3, 127.9, 112.9 (d, *J*_{PC} = 113.3 Hz, 1 C, Ph), 112.8 (17 C, Ph), 66.7 (1 C), 34.8 (1 C, *t*Bu), 26.9 (3 C, *t*Bu) ppm. ³¹P NMR (CDCl₃): δ = 22.4 (d, *J*_{PH} = 474 Hz) ppm. HRMS (EI) calcd. for C₂₃H₂₆NOP [M⁺]: 363.1752; found: 363.1750. Elemental analysis calcd. (%) for C₂₃H₂₆NOP (363.44): C 76.01, H 7.21, N 3.85; found: C 75.66, H 6.64, N 3.55.

Spectroscopic Data for 3b: ¹H NMR (CDCl₃): δ = 7.33–7.23 (m, 8 H), 6.83 (d, *J*_{PH} = 447 Hz, 1 H, P-H), 6.54–6.52 (dd, *J* = 6.4, 2.4 Hz, 2 H), 4.08 (s, 1 H), 1.18 (d, *J*_{PH} = 17.99 Hz, 9 H), 0.96 (s, 9 H) ppm. ¹³C NMR (CDCl₃): δ = 150.9, 140.1, 132.2, 128.3, 127.8, 127.1, 114.0 115.0 (12 C, Ph), 112.6, 66.7 (1 C), 34.8 (1 C, *t*Bu), 32.1 (d, *J*_{PC} = 71.4 Hz, 1 C, *t*Bu), 26.9 (3 C, *t*Bu), 23.4 (3 C, *t*Bu) ppm. ³¹P NMR (CDCl₃): δ = 48.4 (d, *J*_{PH} = 447 Hz) ppm. HRMS (EI): calcd. for C₂₁H₃₀NOP [M⁺]: 343.2065; found 343.2060. C₂₁H₃₀NOP (343.45): calcd. C 73.44, H 8.80, N 4.08; found C 72.70, H 8.55, N 3.68.

Spectroscopic Data for 3c: ¹H NMR (CDCl₃): δ = 7.96 (d, *J*_{PH} = 476 Hz, 1 H, P-H), 7.68–7.27 (m, 9 H), 7.21–7.13 (m, 2 H), 6.65 (dd, *J* = 6.4, 2.4 Hz, 3 H), 4.12 (d, *J*_{PH} = 14.2 Hz, 1 H), 0.99 (s, 9 H) ppm. ¹³C NMR (CDCl₃): δ = 159.7, 151.6, 148.5, 135.7, 132.7, 131.7, 130.6, 128.6, 123.1, 122.0, 116.8 (d, *J*_{PC} = 110.0 Hz, 1 C, Ph), 113.0 (16 C, 2 Ph, py), 66.6 (1 C), 35.6 (1 C, *t*Bu), 26.8 (3 C, *t*Bu) ppm. ³¹P NMR (CDCl₃): δ = 22.4 (d, *J*_{PH} = 476 Hz) ppm. HRMS (EI): calcd. for C₂₂H₂₅N₂OP [M⁺]: 364.1705; found 364.1705. C₂₂H₂₅N₂OP (364.43): calcd. C 72.51, H 6.91, N 7.69; found C 69.06, H 6.90, N 6.82.

Spectroscopic Data for 3d: ¹H NMR (CDCl₃): δ = 8.51 (d, *J* = 4.0 Hz, 1 H, Ar), 7.90 (d, *J* = 8.0 Hz, 1 H, Ar), 7.66 (td, *J* = 7.7, 2.0 Hz, 1 H, Ar), 7.45 (d, *J* = 8.0 Hz, 2 H, Ar), 7.25–7.10 (m, 5 H, Ar), 6.92 (d, *J* = 8.0 Hz, 1 H, Ar), 6.88 (s, 1 H, Ar), 6.87 (d, *J*_{PH} = 512 Hz, 1 H, P-H), 6.81 (dd, *J* = 8.0, 2.4 Hz, 1 H, Ar), 6.23 (d, *J* = 12.4 Hz, 1 H, benzylic), 3.74 (s, 3 H, OCH₃), 0.87 (d, *J*_{PH} = 17.6 Hz, 9 H, *t*Bu) ppm. ¹³C NMR (CDCl₃): δ = 159.7, 159.5, 149.2, 142.3, 140.2, 136.6, 129.7, 129.68, 129.6, 128.9, 126.4, 123.5, 122.5, 122.2, 115.9, 113.6 (17 C, 2 Ph, py), 73.3 (1 C, benzylic), 49.5 (s, OMe), 33.7 (d, *J*_{PC} = 88.0 Hz, 1 C, *t*Bu), 24.6 (3 C, *t*Bu) ppm. ³¹P NMR (CDCl₃): δ = 38.8 (d, *J*_{PH} = 512 Hz) ppm. HRMS (EI): calcd. for C₂₃H₂₇N₂O₂P [M⁺]: 394.1810; found 394.1819. C₂₃H₂₇N₂O₂P (394.45): calcd. C 70.03, H 6.90, N 7.10; found C 69.50, H 6.70, N 6.66.

Spectroscopic Data for 3e: ¹H NMR (CDCl₃): δ = 7.34–7.28 (m, 2 H, Ar), 7.20 (t, *J* = 4.8 Hz, 1 H, Ar), 6.86 (d, *J* = 7.6 Hz, 1 H, Ar), 6.83 (dd, *J*_{PH} = 447 Hz, 1 H, P-H), 6.81 (s, 1 H, Ar), 6.77 (dd, *J* = 5.4, 3.2 Hz, 1 H, Ar), 6.53 (d, *J* = 5.4 Hz, 2 H, Ar), 4.61 (d, *J* = 6.4 Hz, 1 H, Ar), 4.04 (d, *J* = 6.0 Hz, 1 H, benzylic), 3.77 (s, 3 H, OMe), 1.08 (d, *J*_{PH} = 16.8 Hz, 9 H, *t*Bu), 1.00 (s, 9 H, *t*Bu) ppm. ¹³C NMR (CDCl₃): δ = 159.2, 150.9, 141.9, 132.2, 128.8, 121.0, 114.6, 112.7, 111.7 (12 C, 2 Ph), 66.7 (1 C, benzylic), 55.1 (1 C, OMe), 34.9 (1 C, *t*Bu), 32.1 (d, *J*_{PC} = 69.9 Hz, 1 C, *t*Bu), 27.0 (3 C, *t*Bu), 23.5 (3 C, *t*Bu) ppm. ³¹P NMR (CDCl₃): δ = 48.9 (d, *J*_{PH} = 447 Hz) ppm. HRMS (EI): calcd. for C₂₂H₃₂NO₂P [M⁺]: 373.2171; found 373.2178. C₂₂H₃₂NO₂P (373.47): calcd. C 70.75, H 8.64, N 3.75; found C 68.8, H 8.70, N 3.09.

Spectroscopic Data for 3f: ¹H NMR (CDCl₃): δ = 7.50 (d, *J* = 7.6 Hz, 2 H, Ar), 7.13 (m, 2 H, Ar), 7.05 (m, 3 H, Ar), 6.85 (s, 1 H, Ar), 6.79 (s, 1 H, Ar), 6.78 (s, 1 H, Ar), 6.77 (d, *J*_{PH} = 502 Hz, 1 H, P-H), 6.67 (dd, *J* = 5.6, 4.8 Hz, 1 H, Ar), 6.45 (d, *J* = 9.2 Hz, 1 H, benzylic), 3.66 (s, 3 H, OMe), 3.45 (s, 3 H, NMe), 0.94 (d, *J*_{PH} = 18.0 Hz, 9 H, *t*Bu) ppm. ¹³C NMR (CDCl₃): δ = 159.3, 146.3, 141.0, 138.1, 131.3, 129.0, 128.5, 127.2, 126.5, 121.8, 121.1, 114.7, 113.8 (15 C, 2 Ph, imidazole), 57.1 (1 C, benzylic), 55.1 (1 C, -OMe), 34.4 (d, *J*_{PC} = 85.9 Hz, 1 C, *t*Bu), 32.9 (1 C, NMe), 23.6 (3 C, *t*Bu) ppm. ³¹P NMR (CDCl₃): δ = 49.3 (d, *J*_{PH} = 502 Hz) ppm. HRMS (EI): calcd. for C₂₂H₂₈N₃O₂P [M⁺]: 397.1910; found 397.1925. C₂₂H₂₈N₃O₂P (397.46): calcd. C 66.48, H 7.10, N 10.57; found C 67.13, H 7.35, N 10.59.

Spectroscopic Data for 3g: ¹H NMR (CDCl₃): δ = 7.47 (d, *J* = 8.0 Hz, 2 H), 7.26–7.25 (m, 2 H), 7.19–7.11 (m, 5 H), 7.08–7.05 (m, 2 H), 6.82 (s, 1 H), 6.79 (d, *J*_{PH} = 500.1 Hz, 1 H, P-H), 6.51 (d, *J* = 9.2 Hz, 1 H, benzylic), 3.48 (s, 3 H, NCH₃), 0.95 (d, *J* = 17.6 Hz, 9 H, *t*Bu) ppm. ¹³C NMR (CDCl₃): δ = 146.3 (d, *J* = 3.1 Hz), 140.8 (d, *J* = 2.7 Hz), 136.4 (d, *J* = 1.9 Hz), 131.3 (d, *J* = 4.6 Hz), 129.5, 128.4, 128.0, 127.6, 127.1, 126.4, 121.1, 56.6 (d, *J* = 4.5 Hz, benzylic), 34.4 (d, *J*_{PC} = 85.4 Hz, C(CH₃)₃), 32.8 (1 C, NCH₃), 23.5 (d, *J* = 1.6 Hz, CH₃) ppm. ³¹P NMR (CDCl₃): δ = 49.5 (d, *J*_{PH} = 511.3 Hz) ppm. HRMS (EI): calcd. for C₂₁H₂₆N₃OP [M⁺]: 367.1813; found 367.1806. IR (ATR): ν̃ = 2330 (br., P-H), 1489 (P=O) cm⁻¹. C₂₁H₂₆N₃OP (367.43): calcd. C 68.65, H 7.13, N 11.44; found C 66.66, H 6.45, N 9.69.

Spectroscopic Data for 3h: ¹H NMR (CDCl₃): δ = 7.85 (d, *J* = 3.2 Hz, 1 H), 7.36 (t, *J* = 1.6 Hz, 1 H), 7.33–7.31 (m, 2 H), 7.25–7.23 (m, 5 H), 7.19–7.17 (m, 3 H), 6.74 (d, *J*_{PH} = 502.9 Hz, 1 H, P-H), 6.62 (d, *J* =

10.0 Hz, 1 H, benzylic), 1.05 (d, $J = 17.6$ Hz, 9 H, tBu) ppm. ^{13}C NMR (CDCl_3): $\delta = 170.0, 141.9, 140.4, 137.1, 130.6, 129.1, 128.2, 127.6, 127.5, 126.4, 119.6, 63.5$ (1 C, benzylic), 33.8 [d, $J_{\text{PC}} = 86.6$ Hz, $\text{C}(\text{CH}_3)_3$], 23.3 (1 C, CH_3) ppm. ^{31}P NMR (CDCl_3): $\delta = 47.8$ (d, $J_{\text{PH}} = 496.2$ Hz) ppm. HRMS (EI): calcd. for $\text{C}_{20}\text{H}_{23}\text{N}_2\text{OPS}$ [M^+] 370.1269; found 370.1264. IR (ATR): $\tilde{\nu} = 2366$ (br., P–H), 1491 (P=O) cm^{-1} . $\text{C}_{20}\text{H}_{23}\text{N}_2\text{OPS}$ (370.45): calcd. C 64.84, H 6.26, N 7.56; found C 64.36, H 5.93, N 7.23.

Reactions of 3 with Palladium Salts: Under nitrogen, a 20 mL Schlenk tube with magnetic stirrer was charged with THF (2.0 mL), $\text{Pd}(\text{COD})\text{Cl}_2$ (0.029 g, 0.10 mmol), and 2 mol-equiv. of **3f** (0.079 g, 0.20 mmol). The solution was stirred at 60 °C for 16 h before it was cooled to room temperature. Subsequently, the solvent was completely removed under reduced pressure. Then, the residue was dissolved in CH_2Cl_2 (1.0 mL) and purified by column chromatography. The target compound **6f** was obtained in 92.2 % yield (0.053 g, 0.092 mmol). Crystals of **6f** with suitable size for X-ray diffraction were obtained after placing purified **6f** under a two-layered solution (diethyl ether/ CH_2Cl_2) at 4 °C for a few days. The identity of **6f** was determined by spectroscopic means as well as by X-ray diffraction methods. Similar procedures for the preparation of **6g** and **6h** were carried out. The yields of **6g** (pale-yellow solid) and **6h** (bright-yellow solid) were 62 % (0.0336 g, 0.0620 mmol) and 95 % (0.0520 g, 0.0950 mmol), respectively. Crystals of **7fa** and **7fb** were picked out from the results of the crystal-growing process. Since there were no sufficient amounts of compounds **7fa** and **7fb** left for further examination, the spectroscopic analyses of these two compounds are not available. A similar procedure was carried out for the reaction of **3f** (0.079 g, 0.20 mmol) with $\text{Pd}(\text{COD})\text{Cl}_2$ (0.029 g, 0.10 mmol) in 1,4-dioxane at 100 °C for 6 h. The resulting product **8f** was further purified by column chromatography, initially using a mixed solvent (hexanes/ethyl acetate, 1:1) and later pure ethyl acetate. The yield of **8f** was 36.8 % (0.046 g, 0.037 mmol). Suitable crystals for X-ray crystallographic studies were obtained from a two-layered solution (diethyl ether/ CH_2Cl_2).

Spectroscopic Data for 6f: ^1H NMR (CDCl_3): $\delta = 7.66$ (d, $J = 2.0$ Hz, 1 H, Ar), 7.62 (t, $J = 2.4$ Hz, 1 H, Ar), 7.42–7.39 (m, 2 H, Ar), 7.35–7.31 (m, 3 H, Ar), 7.23 (t, $J = 8.0$ Hz, 1 H, Ar), 7.02 (d, $J = 1.6$ Hz, 1 H, Ar), 6.89 (dd, $J = 7.6, 2.0$ Hz, 1 H, Ar), 6.78 (dd, $J = 8.4, 0.8$ Hz, 1 H, Ar), 5.86 (d, $J = 24.0$ Hz, 1 H, benzylic), 3.89 (s, 3 H, OMe), 3.81 (s, 3 H, NCH_3), 0.91 (d, $J_{\text{PH}} = 18.8$ Hz, 9 H, tBu) ppm. ^{13}C NMR (CDCl_3): $\delta = 160.4$ (s), 145.7 (s), 144.3 (s), 138.2 (s), 130.1 (s), 130.0 (s), 128.8 (s), 127.9 (s), 121.6 (s), 119.6 (s), 116.1 (s), 111.8 (s), 67.1 (d, $J_{\text{PC}} = 9.95$ Hz, 1 C, benzylic), 56.1 (s, 1 C, OMe), 40.6 (d, $J_{\text{PC}} = 52.7$ Hz, 1 C, tBu), 34.4 (s, 1 C, NCH_3), 26.0 (d, $J_{\text{PC}} = 5.03$ Hz, 3 C, tBu) ppm. ^{31}P NMR (CDCl_3): $\delta = 112.9$ ppm. HRMS (ESI $^+$): calcd. for $\text{C}_{22}\text{H}_{28}\text{Cl}_2\text{N}_3\text{O}_2\text{PPd}$ [$\text{M} - \text{H}^+$] 573.0331; found 572.0265.

Spectroscopic Data for 6g: ^1H NMR (CDCl_3): $\delta = 7.73$ (d, $J = 1.6$ Hz, 1 H), 7.50–7.48 (m, 2 H), 7.45–7.39 (m, 4 H), 7.38–7.32 (m, 4 H), 7.00 (d, $J = 1.6$ Hz, 1 H), 5.94 (d, $J = 24.0$ Hz, 1 H, benzylic), 3.82 (s, 3 H, NCH_3), 0.91 (d, $J_{\text{PH}} = 18.8$ Hz, 9 H, tBu) ppm. ^{13}C NMR spectroscopic data for **6g** are not available owing to its poor solubility in most commonly used deuterated solvents. ^{31}P NMR (CDCl_3): $\delta = 112.4$ ppm. HRMS (ESI $^+$): calcd. for $\text{C}_{21}\text{H}_{26}\text{Cl}_2\text{N}_3\text{OPd}$ [$\text{M} - \text{H}^+$] 543.0225; found 542.0128.

Spectroscopic Data for 6h: ^1H NMR (CDCl_3): $\delta = 8.57$ (d, $J = 4.0$ Hz, 1 H), 7.61 (d, $J = 3.6$ Hz, 1 H), 7.49–7.40 (m, 9 H), 7.34 (t, $J = 7.2$ Hz, 1 H), 6.27 (d, $J = 24.8$ Hz, 1 H, benzylic), 0.84 (d, $J_{\text{PH}} = 18.8$ Hz, 9 H, tBu) ppm. ^{13}C NMR (CDCl_3): $\delta = 169.3$ (d, $J = 4.5$ Hz), 146.1, 145.1 (d, $J = 6.3$ Hz), 137.9 (d, $J = 2.8$ Hz), 130.2, 129.2 (d, $J = 4.5$ Hz), 127.7, 127.6, 127.2, 71.5 (d, $J = 12.9$ Hz, benzylic), 40.1 [d, $J = 53.2$ Hz, $\text{C}(\text{CH}_3)_3$], 25.9 (d, $J = 4.6$ Hz, CH_3) ppm. ^{31}P NMR (CDCl_3):

$\delta = 109.4$ ppm. HRMS (ESI $^-$): calcd. for $\text{C}_{20}\text{H}_{23}\text{Cl}_2\text{N}_2\text{OPPdS}$ [$\text{M} - \text{H}^+$] 545.9681; found 544.9604.

Spectroscopic Data for 8f: ^1H NMR (CDCl_3): $\delta = 7.80$ (s, 1 H, Ar), 7.51 (d, $J = 8.0$ Hz, 2 H, Ar), 7.32 (t, $J = 7.6$ Hz, 2 H, Ar), 7.19–7.11 (m, 2 H, Ar), 6.88 (s, 1 H, Ar), 6.86 (s, 1 H, Ar), 6.77 (d, $J = 8.0$ Hz, 1 H, Ar), 6.70 (s, 1 H, Ar), 6.01 (d, $J = 18.8$ Hz, 1 H, benzylic), 3.72 (s, 3 H, OMe), 3.68 (s, 3 H, NCH_3), 0.85 (d, $J_{\text{PH}} = 16.0$ Hz, 9 H, tBu), 0.83 (d, $J_{\text{PH}} = 16.0$ Hz, 9 H, tBu) ppm. ^{13}C NMR (CDCl_3): $\delta = 159.7$ (s), 149.0 (s), 146.9 (s), 142.9 (s), 129.8 (s), 129.3 (s), 129.1 (s), 128.7 (s), 124.9 (s), 121.0 (s), 119.8 (s), 114.5 (s), 112.2 (s), 63.9 (d, $J_{\text{PC}} = 8.9$ Hz, 1 C, benzylic), 55.1 (s, 1 C, OMe), 42.4 (d, $J_{\text{PC}} = 50.4$ Hz, 1 C, tBu), 40.4 (d, $J_{\text{PC}} = 54.2$ Hz, 1 C, tBu), 33.3 (s, 1 C, NCH_3), 27.1 (d, $J_{\text{PC}} = 5.3$ Hz, 3 C, tBu), 25.6 (d, $J_{\text{PC}} = 5.3$ Hz, 3 C, tBu) ppm. ^{31}P NMR (CDCl_3): $\delta = 106.1$ (d, $J_{\text{PP}} = 13.8$ Hz), 121.9 (d, $J_{\text{PP}} = 11.5$ Hz) ppm. HRMS (ESI $^+$): calcd. for $\text{C}_{52}\text{H}_{74}\text{N}_6\text{O}_8\text{P}_4\text{Pd}_2$ [$\text{M} + \text{H}^+$] 1246.2588; found 1247.2621. $\text{C}_{52}\text{H}_{74}\text{N}_6\text{O}_8\text{P}_4\text{Pd}_2\cdot\text{C}_4\text{H}_{10}\text{O}$ (1320.33): calcd. C 50.88, H 6.40, N 6.36; found C 51.81, H 6.38, N 5.10.

General Procedure for Catellani Reactions: A nitrogen-filled 20 mL brown Schlenk tube charged with a magnetic stirrer was filled with *N*-(2-bromophenyl)acetamide (0.4 mmol, 0.086 g), $\text{Pd}(\text{OAc})_2$ (0.02 mmol, 5.0 mg), **3h** (0.022 mmol, 8.14 mg), K_2CO_3 (0.8 mmol, 0.111 g), and norbornene (0.42 mmol, 0.040 g). This was processed in a fume hood, and then the tube was capped with a tight seal. The air was pumped out of the tube and replaced by nitrogen. This process was repeated three times. Subsequently, 2-iodotoluene (0.2 mmol, 0.0254 mL) and DMA (2.0 mL) were added under nitrogen. The solution was then heated in an oil bath at 135 °C for 20 h. After that, it was cooled to room temperature, and the resulting products were extracted with water and diethyl ether. The extracted solution was filtered through a flash column and concentrated. Further purification was carried out by centrifugal thin layer chromatography. Finally, the conversion rates of the particular products were analyzed by their distinct chemical shifts using ^1H NMR spectroscopy. Similar procedures were performed when using different ligands such as **3g**, **6h**, PPH_3 , and dppe .

General Procedure for Suzuki–Miyaura Cross-Coupling Reactions: Suzuki–Miyaura cross-coupling reactions were performed according to the following procedures. The four reactants, $\text{Pd}(\text{OAc})_2$, ligand, boronic acid, and base were placed in a suitable, oven-dried Schlenk flask. It was evacuated for 0.5 h and backfilled with nitrogen gas before adding solvent and aryl halide through a rubber septum. The aryl halides, being solids at room temperature, were added prior to the evacuation/backfill cycle. The flask was sealed with a rubber septum, and the solution was stirred at the required temperature for the designated time. Then, the reaction mixture was diluted with ethyl acetate (3 mL) and the cooled solution poured into a separating funnel. The mixture was washed with aqueous NaOH (1.0 M, 5 mL), and the aqueous layer was extracted with ethyl acetate (2×5 mL). The combined organic layers were washed with brine and dried with anhydrous magnesium sulfate. The dried organic layer was concentrated in vacuo. The residue was purified by column chromatography to give the desired product.

X-ray Crystallographic Studies: Suitable crystals of **2x**, **3d**, **3h**, **6f**, **6g**, **6h**, **7fa**, **7fb**, and **8f** were sealed in thin-walled glass capillaries under nitrogen and mounted on a Bruker AXS SMART 1000 diffractometer. Intensity data were collected in 1350 frames with increasing ω (width of 0.3° per frame). The absorption correction was based on symmetry-equivalent reflections by using the SADABS program. The space-group determination was based on a check of the Laue symmetry and systematic absences, and was confirmed by using the structure solution. The structure was solved by direct

methods using a SHELXTL package. All non-H atoms were located from successive Fourier maps, and hydrogen atoms were refined by using a riding model. Anisotropic thermal parameters were used for all non-H atoms, and fixed isotropic parameters were used for H atoms. CCDC 956234 (for **2x**), 956235 (for **3d**), 1401620 (for **3h**), 1401712 (for **6f**), 1401621 (for **6g**), 1401622 (for **6h**), 956238 (for **7fa**), 1401713 (for **7fb**), and 958952 (for **8f**) contain the supplementary crystallographic data for this paper. These data can be obtained free of charge from The Cambridge Crystallographic Data Centre.

Acknowledgments

We thank the Ministry of Science and Technology of the ROC (grant MOST 104-2119-M-005-004) for financial support.

Keywords: Secondary phosphine oxides · Ligand design · Catellani reactions · C–H activation · Palladium · P ligands

- [1] a) J. F. Hartwig, *Organotransition Metal Chemistry, from Bonding to Catalysis*, University Science Books, New York, **2010**; b) R. H. Crabtree, *The Organometallic Chemistry of the Transition Metals*, 5th ed., John Wiley & Sons Inc., Hoboken, **2009**, chapter 4; c) W. Tang, X. Zhang, *Chem. Rev.* **2003**, *103*, 3029–3070; d) J. Hassan, M. Sévignon, C. Gozzi, E. Schulz, M. Lemaire, *Chem. Rev.* **2002**, *102*, 1359–1470; e) N. G. Andersen, B. A. Keay, *Chem. Rev.* **2001**, *101*, 997–1030; f) C. A. Bessel, P. Aggarwal, A. C. Marschilok, K. J. Takeuchi, *Chem. Rev.* **2001**, *101*, 1031–1066.
- [2] S. T. Diver, in *Encyclopedia of Reagents for Organic Synthesis* (Eds.: L. A. Paquette), Wiley, New York, **1995**, vol. 7, pp. 5014–5016.
- [3] R. G. Parr, R. G. Pearson, *J. Am. Chem. Soc.* **1983**, *105*, 7512–7516.
- [4] a) P. Sutram, A. Igau, *Coord. Chem. Rev.* **2016**, *97*, 97–116; b) H. Landert, F. Spindler, A. Wyss, H.-U. Blaser, B. Pugin, Y. Ribourduille, B. Gschwend, B. Ramalingam, A. Pfaltz, *Angew. Chem. Int. Ed.* **2010**, *49*, 6873–6876; *Angew. Chem.* **2010**, *122*, 7025–7028; c) L. Ackermann, H. K. Potukuchi, A. R. Kapdi, C. Schulzke, *Chem. Eur. J.* **2010**, *16*, 3300–3303; d) A. J. Bloomfield, J. M. Qian, S. B. Herzon, *Organometallics* **2010**, *29*, 4193–4195; e) T. Achard, L. Giordano, A. Tenaglia, Y. Gimbert, G. Buono, *Organometallics* **2010**, *29*, 3936–3950; f) C. Li, A. Christiansen, M. Garland, D. Selent, R. Ludwig, A. Spannenberg, W. Baumann, R. Franke, A. Börner, *Eur. J. Org. Chem.* **2010**, 2733–2741; g) L. Ackermann, R. Vicente, N. Hofmann, *Org. Lett.* **2009**, *11*, 4274–4276; h) D. X. Yang, S. L. Colletti, K. Wu, M. Song, G. Y. Li, H. C. Shen, *Org. Lett.* **2009**, *11*, 381–384; i) H. Xu, K. Ekouekovi, C. Wolf, *J. Org. Chem.* **2008**, *73*, 7638–7650; j) K. L. Billingsley, S. L. Buchwald, *Angew. Chem. Int. Ed.* **2008**, *47*, 4695–4698; *Angew. Chem.* **2008**, *120*, 4773–4776; k) L. Ackermann, *Synlett* **2007**, *4*, 507–526; l) J. Bigeault, L. Giordano, I. de Riggis, Y. Gimbert, G. Buono, *Org. Lett.* **2007**, *9*, 3567–3570; m) R. Lerebours, C. Wolf, *J. Am. Chem. Soc.* **2006**, *128*, 13052–13053; n) B. Hoge, P. Garcia, H. Willner, H. Oberhammer, *Chem. Eur. J.* **2006**, *12*, 3567–3574; o) J. Bigeault, L. Giordano, G. Buono, *Angew. Chem. Int. Ed.* **2005**, *44*, 4753–4757; *Angew. Chem.* **2005**, *117*, 4831–4835; p) C. Wolf, R. Lerebours, *Org. Lett.* **2004**, *6*, 1147–1150; q) G. Y. Li, W. J. Marshall, *Organometallics* **2002**, *21*, 590–591; r) G. Y. Li, *J. Org. Chem.* **2002**, *67*, 3643–3650; s) T. Appleby, J. D. Woollins, *Coord. Chem. Rev.* **2002**, *235*, 121–140; t) G. Y. Li, US Patent 6124462, **2000**; WO01040147, **2001**; WO01079213, **2001**; WO02000574, **2002**; u) G. Y. Li, *Angew. Chem. Int. Ed.* **2001**, *40*, 1513–1516; *Angew. Chem.* **2001**, *113*, 1561–1564; v) G. Y. Li, G. Zheng, A. F. Noonan, *J. Org. Chem.* **2001**, *66*, 8677–8681; w) P. L. Polavarapu, F. Wang, *J. Org. Chem.* **2000**, *65*, 7561–7565; x) D. M. Roudhill, R. P. Sperline, W. B. Beaulieu, *Coord. Chem. Rev.* **1978**, *26*, 263–279; y) B. Walther, *Coord. Chem. Rev.* **1984**, *60*, 67–105.
- [5] a) A. J. Bloomfield, S. B. Herzon, *Org. Lett.* **2012**, *14*, 4370–4373; b) T. M. Shaikh, C.-M. Weng, F.-E. Hong, *Coord. Chem. Rev.* **2012**, *256*, 771–803; c) B. Kurscheid, L. Belkoura, B. Hoge, *Organometallics* **2012**, *31*, 1329–1334; d) W. B. Beaulieu, T. B. Rauchfuss, D. M. Roundhill, *Inorg. Chem.* **1975**, *14*, 1732–1734; e) W. B. Farnham, R. A. Lewis, R. K. Murray, K. Mislow, *J. Am. Chem. Soc.* **1970**, *92*, 5808–5809; f) T. L. Emmick, R. L. Letsinger, *J. Am. Chem. Soc.* **1968**, *90*, 3469–3465; g) R. H. Williams, A. Hamilton, *J. Am. Chem. Soc.* **1955**, *77*, 3411–3412; h) R. H. Williams, A. Hamilton, *J. Am. Chem. Soc.* **1952**, *74*, 5418–5420; i) G. M. Kosolapoff, R. M. Watson, *J. Am. Chem. Soc.* **1951**, *73*, 4101–4102.
- [6] a) D.-F. Hu, C.-M. Weng, F.-E. Hong, *Organometallics* **2011**, *30*, 1139–1147; b) L.-Y. Jung, S.-H. Tsai, F.-E. Hong, *Organometallics* **2009**, *28*, 6044–6053; c) C.-H. Wei, C.-E. Wu, Y.-L. Huang, R. G. Kultyshev, F.-E. Hong, *Chem. Eur. J.* **2007**, *13*, 1583–1593.
- [7] a) M. Liniger, B. Gschwend, M. Neuburger, S. Schaffner, A. Pfaltz, *Organometallics* **2010**, *29*, 5953–5958; b) G. Helmchen, A. Pfaltz, *Acc. Chem. Res.* **2000**, *33*, 336–345.
- [8] a) L. Ackermann, A. R. Kapdi, S. Fenner, C. Korhaß, C. Schulzke, *Chem. Eur. J.* **2011**, *17*, 2965–2971; b) L. Ackermann, R. Born, *Angew. Chem. Int. Ed.* **2005**, *44*, 2444–2447; *Angew. Chem.* **2005**, *117*, 2497–2500.
- [9] P. A. Donets, N. Cramer, *J. Am. Chem. Soc.* **2013**, *135*, 11772–11775.
- [10] a) R. Ghosh, N. N. Adarsh, A. Sarkar, *J. Org. Chem.* **2010**, *75*, 5320–5322; b) L. Ackermann, H. K. Potukuchi, A. Althammer, R. Born, P. Mayer, *Org. Lett.* **2010**, *12*, 1004–1007; c) C. M. So, C. P. Lau, F. Y. Kwong, *Org. Lett.* **2007**, *9*, 2795–2798; d) D. Benito-Garagorri, E. Becker, J. Wiedermann, W. Lackner, M. Pollak, K. Mereiter, J. Kisala, K. Kirchner, *Organometallics* **2006**, *25*, 1900–1913.
- [11] a) Q. Liang, P. Xing, Z. Huang, J. Dong, K. B. Sharpless, X. Li, B. Jiang, *Org. Lett.* **2015**, *17*, 1942–1945; b) J. Magano, S. Monfette, *ACS Catal.* **2015**, *5*, 3120–3123; c) C. Allolio, T. Strassner, *J. Org. Chem.* **2014**, *79*, 12096–12105; d) N. Oger, M. d'Halluin, E. Le Grogne, F.-X. Felpin, *Org. Process Res. Dev.* **2014**, *18*, 1786–1801; e) N. Miyaura, A. Suzuki, *Chem. Rev.* **1995**, *95*, 2457–2483.
- [12] a) M. Catellani, G. P. Chiusoli, A. Mari, *J. Organomet. Chem.* **1984**, *275*, 129–138; b) M. Catellani, G. P. Chiusoli, C. Peloso, *Tetrahedron Lett.* **1983**, *24*, 813–816.
- [13] a) Y. Cheng, C. Bolm, *Angew. Chem. Int. Ed.* **2015**, *54*, 12349–12352; *Angew. Chem.* **2015**, *127*, 12526–12529; b) J. Li, L. Ackermann, *Angew. Chem. Int. Ed.* **2015**, *54*, 8551–8554; *Angew. Chem.* **2015**, *127*, 8671–8674; c) Y. Gao, Y.-B. Huang, W.-Q. Wu, K.-F. Huang, H.-F. Jiang, *Chem. Commun.* **2014**, *50*, 8370–8373; d) D. I. Chai, P. Thansandote, M. Lautens, *Chem. Eur. J.* **2011**, *17*, 8175–8188; e) X. Chen, K. M. Engle, D.-H. Wang, J.-Q. Yu, *Angew. Chem. Int. Ed.* **2009**, *48*, 5094–5115; *Angew. Chem.* **2009**, *121*, 5196–5217; f) R. G. Bergman, *Nature* **2007**, *446*, 391–393; g) K. Godula, D. Sames, *Science* **2006**, *312*, 67–72; h) J. A. Labinger, J. E. Bercaw, *Nature* **2002**, *417*, 507–514; i) C. Jia, T. Kitamura, Y. Fujiwara, *Acc. Chem. Res.* **2001**, *34*, 633–639; j) A. E. Shilov, G. B. Shul'pin, *Chem. Rev.* **1997**, *97*, 2879–2932.
- [14] a) Catellani-type Suzuki reactions: M. Catellani, E. Motti, M. Minari, *Chem. Commun.* **2000**, 157–158; b) Catellani-type Heck reactions: M. Catellani, F. Frignani, A. Rangoni, *Angew. Chem. Int. Ed. Engl.* **1997**, *36*, 119–122; *Angew. Chem.* **1997**, *109*, 142–145.
- [15] a) E. Motti, F. Faccini, I. Ferrari, M. Catellani, R. Ferraccioli, *Org. Lett.* **2006**, *8*, 3967–3970; b) M. Catellani, S. Deledda, B. Ganchegui, F. Hénin, E. Motti, J. Muzart, *J. Organomet. Chem.* **2003**, *687*, 473–482; c) M. Catellani, E. Motti, B. Simone, *Org. Lett.* **2001**, *3*, 3611–3614; d) M. Catellani, E. Motti, L. Paterlini, *J. Organomet. Chem.* **2000**, *593*–594, 240–244; e) M. Catellani, F. Cugini, *Tetrahedron* **1999**, *55*, 6595–6602.
- [16] a) Z. Qureshi, H. Weinstabl, M. Suhartono, H. Liu, P. Thesmar, M. Lautens, *Eur. J. Org. Chem.* **2014**, 4053–4069; b) A. Rudolph, N. Rackelmann, M. Lautens, *Angew. Chem. Int. Ed.* **2007**, *46*, 1485–1488; *Angew. Chem.* **2007**, *119*, 1507–1510.
- [17] a) E. Motti, N. D. Cá, D. Xua, S. Armani, B. M. Aresta, M. Catellani, *Tetrahedron* **2013**, *69*, 4421–4428; b) D. A. Candito, M. Lautens, *Angew. Chem. Int. Ed.* **2009**, *48*, 6713–6716; *Angew. Chem.* **2009**, *121*, 6841–6844; c) C. Blaszykowski, E. Aktoudianakis, D. Alberico, C. Bressy, D. G. Hulcoop, F. Jafarpour, A. Joushaghani, B. Laleu, M. Lautens, *J. Org. Chem.* **2008**, *73*, 1888–1897; d) P. Thansandote, D. G. Hulcoop, M. Langer, M. Lautens, *J. Org. Chem.* **2009**, *74*, 1673–1678; e) D. I. Chai, M. Lautens, *J. Org. Chem.* **2009**, *74*, 3054–3061; f) D. A. Candito, M. Lautens, *Org. Lett.* **2010**, *12*, 3312–3315.
- [18] Structurally related compounds were reported; for details, see: a) Y.-Y. Chang, F.-E. Hong, *Tetrahedron* **2013**, *69*, 2327–2335; b) L.-Y. Jung, S.-H. Tsai, F.-E. Hong, *Organometallics* **2009**, *28*, 6044–6053; c) R. B. Bedford,

S. L. Hazelwood, M. E. Limmert, J. M. Brown, S. Ramdeehul, A. R. Cowley, S. J. Coles, M. B. Hursthouse, *Organometallics* **2003**, 22, 1364–1371; d) A. M. Z. Slawin, M. Wainwright, J. D. Woollins, *J. Chem. Soc., Dalton Trans.* **2001**, 2724–2730; e) A. M. Z. Slawin, M. Wainwright, J. D. Woollins, *New J. Chem.* **2000**, 24, 69–71; f) D. Matt, F. Ingold, F. Balegroune, D. Grandjean, *J. Organomet. Chem.* **1990**, 399, 349–360.

[19] N. D. Cá, G. Sassi, M. Catellani, *Adv. Synth. Catal.* **2008**, 350, 2179–2182.

Received: February 23, 2016

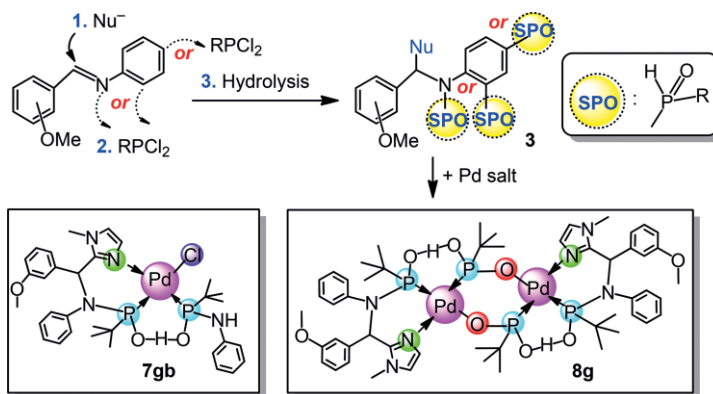
Published Online: ■

Pd Catalysts

C.-Y. Hu, Y.-Q. Chen, G.-Y. Lin,
M.-K. Huang, Y.-C. Chang,
F.-E. Hong* 1–13



Preparation of Secondary Phosphine Oxide Ligands through Nucleophilic Attack on Imines and Their Applications in Palladium-Catalyzed Catellani Reactions



Several new secondary phosphine oxide (SPO) type ligands, **3a–3n**, were prepared. In addition, some SPOs as well as coordinated palladium complexes of ligand **3f**, that is, **7fa**, **7fb**,

and **8f**, with fascinating bonding modes were characterized by X-ray diffraction methods. Some of these ligands were chosen to assist in palladium-catalyzed Catellani reactions.

DOI: 10.1002/ejic.201600181